APPLICATION OF FOREST RESOURCE MANAGEMNET USING ALOS PALSAR DATA

PI No 3140002
Masato KATHO
Faculty of Agriculture, Shinshu University
8304 Minamiminowa-Vill. Kamiina-Dtrct. Nagano 399-4598 Japan
E-mail mkatoh@shinshu-u.ac.jp

1. INTRODUCTION

Sustainable management of the world's forest resources is one of the most pressing environmental issues of our time. Passive remote sensing systems record electromagnetic energy, i.e., reflected visible and near-infrared light or emitted thermal infrared energy radiation from the surface of the Earth. In contrast, active microwave remote sensing systems are not dependent on visible light or the Earth's thermal properties, and are based on transmission of long-wavelength microwave radiation, through the atmosphere and record the amount of backscatter from the terrain or Earth objects (Jensen, 2007). Active radar remote sensing with Synthetic Aperture Radar (SAR) offers the possibility of imaging at a scale large enough to produce regional datasets that are comparable to optical satellite data. Since the successful launch of the Advanced Earth Observing Satellite with Phased Array L-band Synthetic Aperture Radar (ALOS/PALSAR), a great deal of attention has been paid to polarimetric radar remote sensing. This method is expected to contribute to monitoring global forest conditions (Shimada et al., 2008). There has been little SAR research on Japanese forests because forestry scientists who mostly use optical sensor analysis find it difficult to make sense of the physical theory of radar or SAR. They rarely specify SAR software for preparing data analysis, speckle noise reduction, classification, etc.. Now, polarimetric SAR data processing and an educational toolbox, PolSARpro, have been developed by the European Space Agency. Moreover some polarimetric SAR satellites and airborne sensor data are now available. Table 1 provides characteristics of major current satellite radar sensors. ALOS/PALSAR is the first L-band polarimetric SAR sensor on a satellite in the world. In general, shorter wavelengths (2 to 6 cm) are best for sensing agricultural crop canopies (corn, soybean, wheat, etc.) and tree leaves. However, poor atmospheric weather conditions, such as clouds and rain, confine radar signals to a shorter operating wavelength (less than 4 cm). Longer wavelengths (10 to 30 cm) are best for sensing tree trunks and branches (Lillesand et al., 2004); therefore the L band (15 to 30 cm) of the ALOS/PALSAR sensor may be appropriate for determining forest cover type or structural monitoring, because the radar can penetrate tree leaves and canopies. We investigated and verified the usefulness of polarimetric PALSAR data in forests.

2. STUDY AREA and METHODS

The study area is a forested region on the southern slope of Mt. Asama in Nagano Prefecture, at the center of Honshu Island, Japan. Mt. Asama is an active complex volcano in central Honshu, the main island of Japan. Mt. Asama erupted most recently on 2 February 2009, spewing hot rocks and ash up to 2 km. The study area is a suitable site for SAR analysis because of its geographic features, with a wide range of gentle slopes and pure conifer plantations. The summit of Mt. Asama [2568 m above sea level (asl)] is exposed gravel, the sub-alpine area (≤ 1500 m asl) contains *Abies mariesii* and *Tsuga diversifolia*, and the foothills

(800–1500 m asl) are covered with *Larix kaempferi*, *Pinus densifolia*, and other conifer and broadleaf trees (Fig. 1). *Larix kaempferi* plantations are found in many parts of Japan and include the oldest man-made forest (180 years-old) in Japan.

The forest compartment boundaries of national and private forest ownership were overlaid on the study site (Fig. 2). The forest is mainly composed of conifer plantations dominated by *L. kaempferi* and *P. densifolia*, with some broadleaf trees.

The PALSAR data of ALOS in polarimetric mode were acquired for 24 February 2007, during snowy and cloudy weather, and at 21.5° off-nadir.

The flow chart in Fig. 3 provides an overview of the methods used. Image processing and analysis were performed using SAR processing with POLSARpro ver. 4.0 (European Space Agency), the forest cover map based on GIS data was processed with ARCGIS ver. 9.0 (ESRI, 2005), and geometric correction processing was performed using ERDAS IMAGINE ver. 8.6 (Geosystems, 2007).

Fig. 1 Study area
Mt. Asama on 24 December 2008. Location of the study area on Mt. Asama, Nagano Prefecture, central Honshu Island, Japan

3. Results and Discussion

We extracted the study area from the acquired SAR data. Original data were converted into coherent matrices in the form of a three-element target vector in which the elements were associated with the polarimetric channels HH, VV, and HV. The Pauli color-coded image was based on a vector representation of linear combinations of scattering matrix elements. The image was produced with polarimetric channels HH+VV, HH-VV, and HV, which were then associated with the colors blue, red, and green, respectively (Fig. 4a). This image was created by the ALOS satellite flying from north to south for descending path, and equipped with the PALSAR sensor, which faced west. In addition, noise over homogeneous areas was reduced using typical Lee Speckle filtering (Lee et al., 2009); noise that is characteristic of a SAR radar image is removed (Fig. 4b), thus making it easier to interpret geographical features and land cover. Several interpretations were derived from the Pauli color images of the forest areas around Mt. Asama. Green indicated a dominant HV component, characteristic of vegetated areas and implying wave volume scattering. The blue color over the gravel area on Mt. Asama or bare soil in fields indicated that the magnitude of the first polarimetric channels, HH+VV, was large compared to that of the other channels, denoting single wave bounce scattering. White or red coloration over residential areas indicated the dominance of HH-VV, implying double wave bounce scattering. Some black areas were found over the lake and crater of Mt. Asama because there was little scattering. On the other hand, north-south running ridges were white because of strong scattering of the radar signal, as the satellite was flying north to south with the PALSAR looking west.

We conducted a field survey with the Pauli color images and aerial photos to select training areas with different land cover classes as reference data. We found that the vegetation color of forested areas (green) differed from that

of pastures and a golf course (blue). There was also a tonal difference in fields, because some rice fields were waterlogged.

Coherent decomposition was applied to represent all the polarimetric information in a full polarimetric SAR image using the H–A–A (Entropy–Anisotropy–Alpha) method. The image was automatically divided into 16 classes using unsupervised Wishart H–A–A classification (Fig. 5a). Some clusters were merged during interpretation of the image, because classified clusters separated the same area into several distinct clusters. The forest area was defined by combining four tree cover types (Fig. 5b). This procedure was useful for extracting the forest area. Supervised classification divided the forest area into *L. kaempferi*, *P. densifolia*, *A. mariessii*, and broadleaf trees (Fig. 6). The confusion matrix of classification accuracy is shown in Table 2, where boldface diagonal values indicate the numbers of samples in each class that were classified correctly. Producer and user accuracy were calculated from this table. The overall accuracy of the classification was 31% (11590 out of 37378 samples classified correctly) in all training areas, with 40.4% of *L. kaempferi* and 41.6% of *P. densifolia* correctly identified. The accuracy of classifying broadleaf trees was the lowest (11.0%), because the leaves had dropped from the deciduous trees.

The study area was also divided into volume classes using a supervised classification based on ancillary data (Fig. 7). High volume stands were located at the foothill and west parts of Mt. Asama, because these sites were attributed to good condition for *L. kaempferi* growth. The highest volume classes were 301–450 m^3/ha (56.5%) and 451–800 m^3/ha (49.6%,), followed by 0–50 m^3/ha (22.0%), 51–150 m^3/ha (17.7%), and 151–300 m^3/ha (7.7%) in Table 3. This result may represent the estimation capacity for forest biomass using PALSAR data in high-volume stands.

Finally, the classified image was precisely positioned using ground control points and was rectified by geometric correction. A forest cover 3D map was produced with the overlaid GIS data (Fig. 8) showing that *L. kaempferi* and *P. densifolia* were dominant on southern and western slopes. This image, in combination with high-spatial resolution imagery, LiDAR, etc., is useful for forest officers to capture forest conditions (Goodenough et al., 2008, Hiker et al., 2008, Katoh et al., 2009, Treuhaft, et al., 2004).

PALSAR data were more influenced by slope azimuth and mountainous geographic and object features than by forest cover type. Forest cover classification based on polarimetric PALSAR data for trees without leaves could only be acquired in the appropriate seasons in deciduous broadleaf forest. Further application and testing are needed to extend our results to other sites, multiple scenes, and different forest conditions.

6. REFERENCES

[1] ARCGIS 9.0 (2005) What is ARCGIS 9.1, ESRI Co, Redlands, California, 123pp.

[2] ERDAS IMAGINE 8.6 http://gi.leica-geosystems.com/default.aspx Cited Oct.2007.

[3] Goodenough, D.G. Niemann, K.O. Dyk, A. Hobart, G. Gordon, P. Loisel, M. and Hao, C. (2008) Comparison of AVIRIS and AISA airborne hyperspectral sensing for above-ground forest carbon mapping. Proc. IGARSS'08, Boston, II-129-132

[4] Hilker, T. Wulder, M.A. and Coops, N.C. (2008) Update of forest inventory data with LiDAR and high spatial resolution satellite data. Can. J. Remote sensing, 34(1):5-12

[5] Lillesand, T. M. Kiefer, R.W and Chipman, J.W (2004) Remote sensing and Image interpretation. Fifth edition. John Wiley & Sons, NJ, 638-738.

[6] Lee, J.E and Pottier, E (2009) Polarimetric radar imaging from basic to applications. CRC Press, NJ, 398pp.

[7] Jensen, J. R. (2007) Remote sensing of the environment: An earth resource perspective. 2nd edition, Prentice-Hall, Englewood Cliffs, New Jersey, 291-330.

[8] Katoh, M. Gougeon, F.A. and Leckie D.G. (2009) Application of high-resolution airborne

data using individual tree crowns in Japanese conifer plantations. Journal of Forestry Research 14(1):10-19

[9] Katoh, M. Iisaka J., (2009) Forest cover type classification at Mt. Asama using ALOS fully Polarimetric PALSAR data, in Nagano prefecture, central Japan, Jpn PE&RS 48(3):188-194, 2009.

[10] Katoh, M. (2010) Individual large tree identification using ALOS PRISM data, "Forest remote sensing in Japan – from basics to applications" JFIC, Tokyo, pp.308-309, 2010.

[11] POLSARpro http://earth.esa.int/polsarpro/ European Space Agency

[12] Shimada, M. Isoguchi, O. and Rosenqvist, R. (2008) PALSAR CALVAL and generation of the continent scale mosaic products for Kyoto carbon projects. Proc. IGARSS'08, Boston, I - 17-20

[13] Treuhaft, RN. Law, BE. and Asner, GP. (2004) Forest attributes from radar interferometric structure and its fusion with optical remote sensing. Bioscience 54(6):561-571

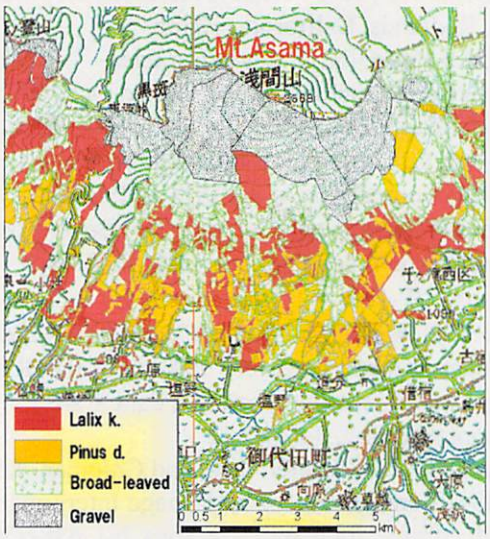

Fig. 2 GIS forest cover type map

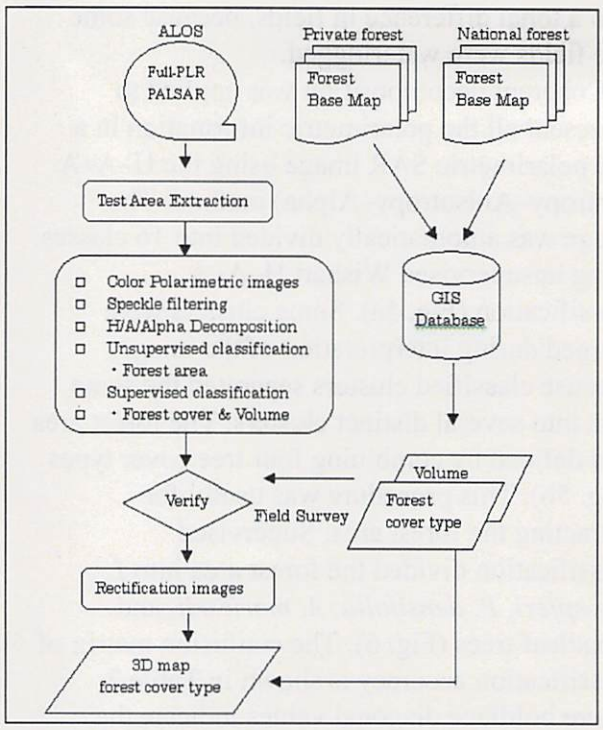

Fig.3 Flow chart

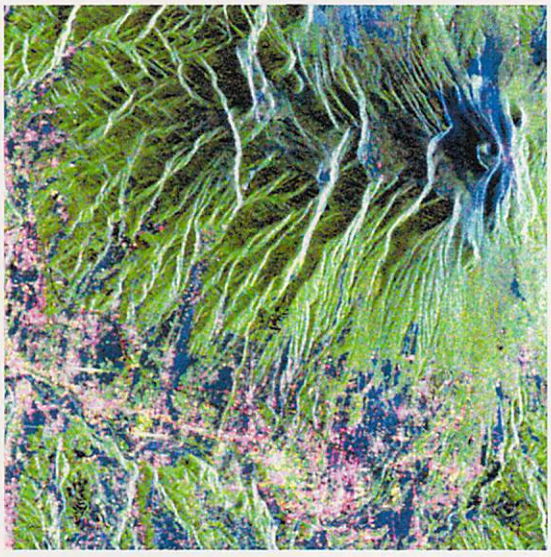

Fig. 4 Pauli color-coded fully polarimetric PALSAR image
Upper: Pauli color image, lower: Speckle filtered image.

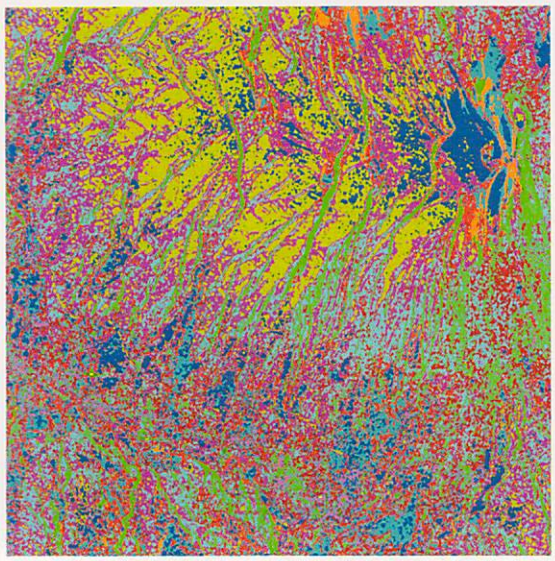

Fig-5 Unsupervised Wishart H-A-A classification
Upper: Wishart H–A–A segmentation into 16 classes, lower: Forest area.

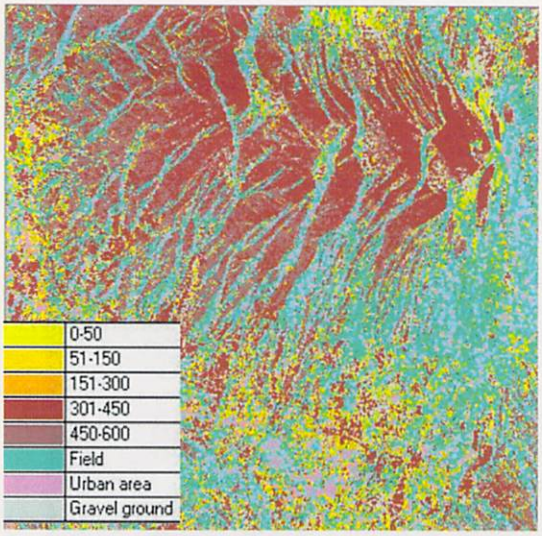

Fig. 6 Forest cover type image with a supervised classification

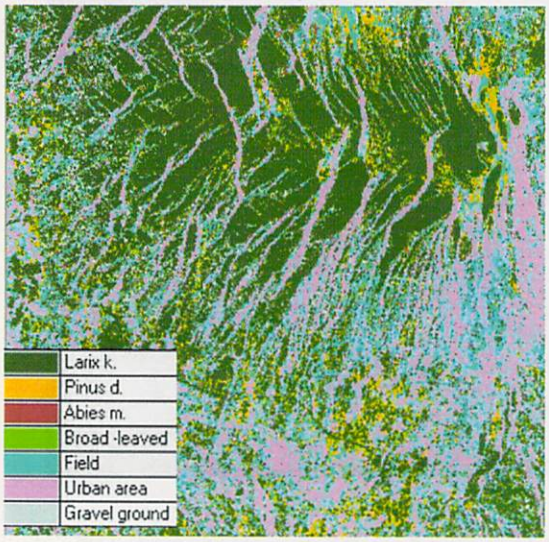

Fig. 7 Volume image with a supervised classification

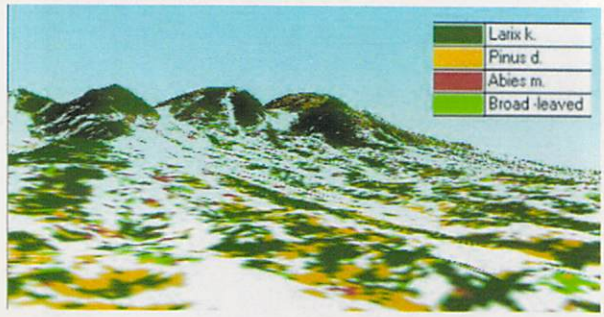

Fig. 8 Forest cover type map with 3D display corresponding to Fig.1

Table1 Characteristics of the current satellite radar sensor

Satellite name	Envisat	ALOS	Radarsat-2	TerraSAR-X
Country*	Europe	Japan	Canada	Germany
Launch date	Mar. 1, 2002	Jan. 24, 2006	Dec. 14, 2007	Jun. 15, 2007
Radar sensor	ASAR	PALSAR	Commercial SAR	Commercial SAR
Wavelength band	C band	L band	C band	X band
Wavelength (cm)	5.63	23.62	5.55	3.02
Frequency (MHz)	5330	1270	5405	9950
Polarization mode	Single ,Dual	Single, dual, quad	Single, dual, quad	Single, dual, quad
Polarizations	HH,VV,HV,VH	HH,VV,HV,VH	HH,VV,HV,VH	HH,VV,HV,VH
Swath width (km)	5-406	30-350	10-500	10-200
Resolution (m)	30-1000	10-100	3-100	1-30

*: Country/International Organization

Table 2. Confusion matrix for classification accuracy of forest cover types

	Forest cover type								User's
Land cover type	Lk	Pd	Am	Bl	F	U	G	Total	Accuracy
Larix kaempferi (Lk)	**2122**	731	21	342	209	798	1030	5253	40.4%
Pinus densiforia (Pd)	1934	**4322**	48	1193	870	874	1156	10397	41.6%
Abies mariessii (Am)	1173	448	**529**	284	145	226	711	3016	17.5%
Broad -leaved (Bl)	2133	1507	36	**660**	207	524	954	6021	11.0%
Field (F)	944	444	129	104	**827**	665	315	3428	24.1%
Urban area (U)	212	132	146	62	816	**1980**	162	3510	56.4%
Gravel ground (G)	2305	766	195	188	798	351	**1150**	5753	20.0%
Total	10823	8350	1104	2833	3872	5418	5478	37378	
Producer's accuracy	20%	52%	48%	23%	21%	37%	21%		**31%**

Table 3. Confusion matrix for classification accuracy of volume classes

	Volume class									User's
Volume class (m3/ha)	0-50	51-150	151-300	301-450	451-800	F	U	G	Total	Accuracy
0-50	441	177	94	298	181	346	159	305	2001	22.0%
51-150	105	240	25	272	208	218	28	261	1357	17.7%
151-300	204	54	134	338	57	401	278	282	1748	7.7%
301-450	73	68	10	1233	246	181	124	249	2184	56.5%
451-800	22	26	0	505	755	95	77	61	1541	49.0%
Field (F)	358	80	111	172	208	1222	583	312	3046	40.1%
Urban area (U)	103	39	88	49	30	482	484	97	1372	35.3%
Gravel ground (G)	342	279	69	806	975	624	103	608	3806	16.0%
Total	1648	963	531	3673	2660	3569	1836	2175	17055	
Producer's accuracy	27%	25%	25%	34%	28%	34%	26%	28%		30%